

Electrochemical Behavior of the Oxygen Radical. IV. The Reaction Mechanism of the Electrogenerated Hyperoxide Ion with Bis(acetylacetonato)cobalt(II) in Dimethyl Sulfoxide and Acetone[†]

Setsuko KUDO^{††} and Akio IWASE*

Department of Chemistry, Faculty of Science, Yamagata University, Yamagata 990

(Received March 27, 1978)

The reaction mechanism of the electrogenerated hyperoxide ion with bis(acetylacetonato)cobalt(II) in dimethyl sulfoxide and acetone has been investigated. The reaction was conducted in a 0.05 mol dm⁻³ TBAP solution at 20 °C in an open system. Co(acac)₂ reacted with the hyperoxide ion which was generated by the controlled potential electrolysis of dissolved oxygen to afford the following product, [(acac)₂Co-O₂-Co(acac)₂]²⁻. The complex was separated in solution by column chromatography using alumina as the adsorbent. The electronic spectrum and oxidation state are discussed.

In Part III of this series,¹⁾ the mechanism of the polarographic catalytic reduction of dissolved oxygen in dimethyl sulfoxide in the presence of bis(1,3-diketono)cobalt(II) complexes was discussed. In this paper, the reaction mechanism of bis(acetylacetonato)cobalt(II) complex, Co(acac)₂ with electrogenerated hyperoxide ion in dimethyl sulfoxide (DMSO) and acetone will be reported in more detail. Moreover, the reaction product, μ -peroxo-dicobalt(II) complex, has been separated by column chromatography using alumina as an adsorbent.

Experimental

Apparatus and Reagents. D.c. polarograms were recorded with a PA 101 Yanagimoto Polarograph and a PT-P8 Yanagimoto Potentiostat, by the same procedures as described in a preceding paper.¹⁾ The capillary used had an *m* value of 1.057 mg/s and drop time of 5.1 s/drop at -1.0 V vs. SCE when measured in an air-free 0.05 mol dm⁻³ TBAP(tetrabutylammonium perchlorate)-DMSO solution at 49 cm of effective height of mercury ($m^{2/3} t^{1/6} = 1.364 \text{ mg}^{2/3} \text{ s}^{-1/2}$).

Cyclic voltammetric measurements were made with a three-electrode potentiostat constructed with a LS-LC Hokuto Denko Linear Scanner and a PT-P8 Yanagimoto Potentiostat. The voltammograms were recorded on a F-32 Riken Denshi X-Y plotter. The working electrode for cyclic voltammetry was a hanging mercury drop electrode (surface area: 0.033 cm²).

A VE-8 Yanagimoto Controlled Potential Electrolyser was used for the controlled potential electrolysis of dissolved oxygen, at -1.15 V vs. SCE at room temperature (ca. 20 °C). For the controlled potential electrolyses, a mercury pool electrode was used as cathode. The electrolytic cell was the same as reported previously.²⁾

The electronic spectra were measured with a Spectronic 88-UV Shimadzu-Bausch & Lomb spectrophotometer.

All voltammetric measurements were conducted at (25 ± 0.2) °C.

Bis(acetylacetonato)cobalt(II) and tris(acetylacetonato)cobalt(III) complexes of reagent grade were obtained from Dojin Yakukagaku Kenkyusho. DMSO(Wako Pure Chemical) and acetone (Koso Chemical), guaranteed reagents

were used without further purification (water contents were below 0.2%). TBAP for polarography from Nakarai Chemicals was used as the supporting electrolyte.

The alumina used for the chromatographic separation of the reaction product was Alumina 60(Merk). The separation of reaction product was carried out by using an alumina column of diameter 1.2 cm and height 30 cm.

Procedure. The solution for controlled potential electrolysis (40 cm³), containing 2×10^{-3} mol dm⁻³ Co(acac)₂ and 0.05 mol dm⁻³ TBAP in DMSO(B) or acetone(A), was placed in an electrolytic cell and electrolyzed for 18 min on a mercury pool electrode. Subsequently the electrolyzed solution was transferred to a clean flask and allowed to stand overnight at room temperature. This solution (30 cm³) was fed into the top of the column bed, which had been washed with acetone or DMSO. The column was operated by the usual chromatographic procedures. In the case of solution A, one of the green complexes, A-1, was eluted with acetone and the other green complex, A-2, was eluted with DMSO. In the case of solution B, the major part of the green complex, B-1, was eluted with DMSO. In both cases, some original complex remained on top of the column under these conditions.

The eluates were used for the polarographic and the spectrophotometric measurements because of the difficulty of preparing crystals.

Results and Discussion

The typical cyclic voltammograms of dissolved oxygen in acetone and DMSO with 0.05 mol dm⁻³ TBAP are shown in Fig. 1. The rate of voltage change was 0.05 V/s. The experimental results were very similar to that reported by earlier investigators.³⁾ Curve 2 and curve 4 represent cyclic voltammograms for oxygen in the presence of Co(acac)₂. It is clear that the heights of cathodic peaks in both cases are larger than those of curves 1 and 3. This catalytic current is clearly based on the reduction of oxygen which is reproduced from the reaction of hyperoxide ion with Co(acac)₂ complex at the electrode surface. Conversely, the heights of the anodic peaks decreased by the addition of the complex.

For the controlled potential electrolysis in acetone and DMSO, the reaction was followed by taking the visible spectrum of the solution at different times. Those spectra are shown in Figs. 2 and 3. In Fig. 2, curve 1 was obtained from a solution containing 2×10^{-3} mol dm⁻³ Co(acac)₂ and 0.05 mol dm⁻³ TBAP in DMSO before electrolysis. The spectrum consists of

[†] A preliminary report of this work was presented at the 36th National Meeting of the Chemical Society of Japan, Osaka, April 1977.

^{††} Present address: Chemical Laboratories, Yamagata Building Service Co., Ltd., Yamagata 990.

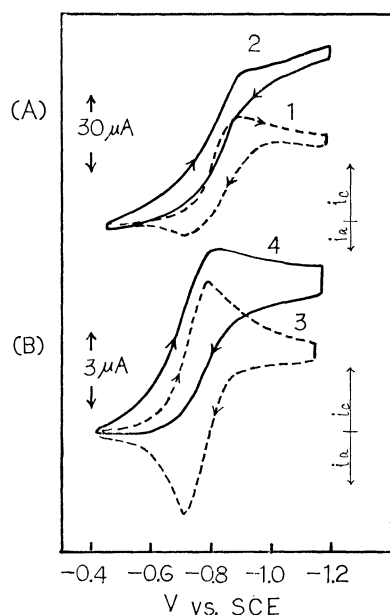


Fig. 1. Cyclic voltammograms of dissolved oxygen in (A) acetone and (B) DMSO.

The concentration of $\text{Co}(\text{acac})_2$ added: (1) and (3), 0; (2), $1.5 \times 10^{-3} \text{ mol dm}^{-3}$; (4), $1.9 \times 10^{-3} \text{ mol dm}^{-3}$.

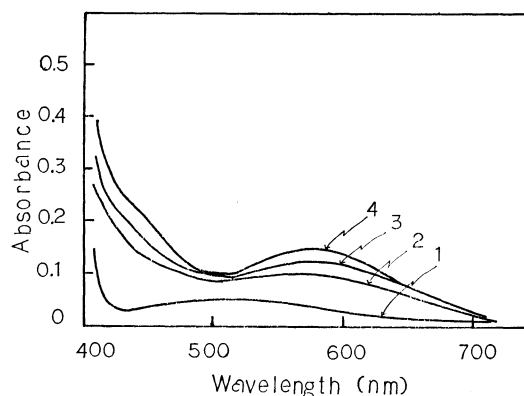


Fig. 2. Electronic spectra of Co(II) complexes in DMSO.

- 1: $2 \times 10^{-3} \text{ mol dm}^{-3} \text{ Co}(\text{acac})_2$,
- 2: solution (1) electrolyzed for 20 min at -1.15 V vs. SCE,
- 3: solution (2) after 5 h at room temperature,
- 4: solution (2) after 6 d at room temperature.

a peak split at 520 and 510 nm (molar absorption coefficient: $\epsilon = 30 \text{ dm}^3 \text{ mol}^{-1} \text{ cm}^{-1}$), which corresponds to ${}^4\text{T}_{1g}(\text{F}) \rightarrow {}^4\text{T}_{1g}(\text{P})$.⁴⁾ For curves 2, 3, and 4 a new strong peak appeared in the neighbourhood of 590 nm with a shoulder at 440 nm, and the intensity increased with respect to the time after electrolysis. In the case of acetone, the spectrophotometric profile of the solution after electrolysis also showed a similar tendency (Fig. 3). The new absorption band in Figs. 2 and 3 can be attributed to the absorption of the μ -peroxo-dicobalt(II) complex, formed by the disproportionation of the $\text{Co}(\text{acac})_2\text{O}_2^-$ complex in acetone or DMSO (Scheme 1).

In Fig. 4, curves 1 and 2 are shown for complexes A-1 and B-1. In curve 1, the absorption peak appeared

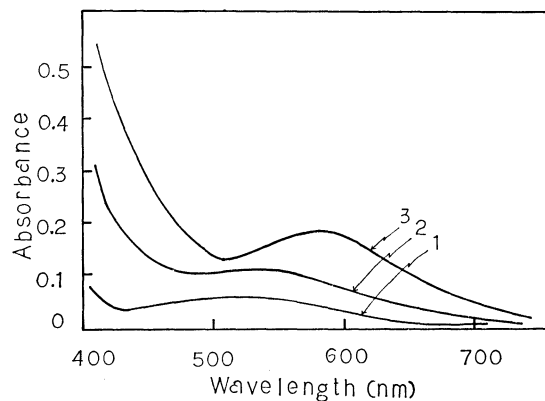


Fig. 3. Electronic spectra of Co(II) complexes in acetone.

- 1: $2 \times 10^{-3} \text{ mol dm}^{-3} \text{ Co}(\text{acac})_2$,
- 2: solution (1) electrolyzed for 18 min at -1.15 V vs. SCE,
- 3: solution (2) after 17 h at room temperature.

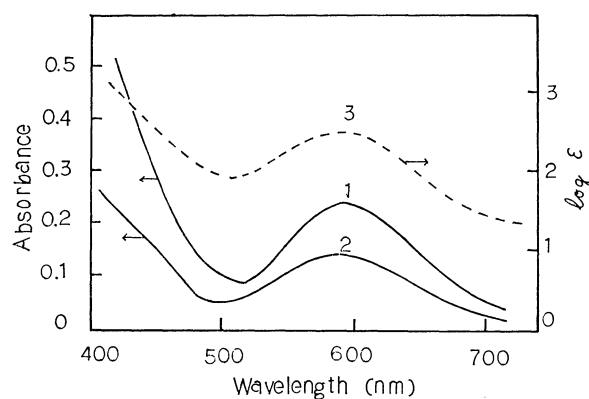


Fig. 4. Electronic spectra of Co(II) complexes.

- 1: $[(\text{acac})_2\text{Co}-\text{O}_2-\text{Co}(\text{acac})_2]^{2-}$ in acetone,
- 2: $[(\text{acac})_2\text{Co}-\text{O}_2-\text{Co}(\text{acac})_2]^{2-}$ in DMSO,
- 3: $[(\text{dpm})_2\text{Co}-\text{O}_2-\text{Co}(\text{dpm})_2]^{2-}$ in acetone.

at 597 nm in acetone and in curve 2, at 590 and 440 nm (shoulder) in DMSO. The band widths were usually about 110 nm. The molar absorption coefficients are unknown since it is difficult to obtain the solids. Attempts to isolate the μ -peroxodicobalt(II) complex as crystals were unsuccessful for two reasons: (1) increasing the time of electrolysis did not change the yield and (2) the complex was not obtained by TBAP and consequently difficult to crystallize under the experimental conditions. In the case of the $\text{Co}(\text{dpm})_2$ complex, however, the $[(\text{dpm})_2\text{Co}-\text{O}_2-\text{Co}(\text{dpm})_2]^{2-}$ complex was isolated as crystals⁵⁾ (dpm represents an anion of dipivaloylmethane). The molar absorption coefficient and band width of the peak at 588 nm was $410 \text{ dm}^3 \text{ mol}^{-1} \text{ cm}^{-1}$ and 110 nm respectively (curve 3 in Fig. 4).

It is well documented that the most common geometry of ligands around the cation in the high spin state cobalt(II) complex are octahedral, square pyramidal, and tetrahedral. Generally in an octahedral field, there are two d-d absorption bands at approximately 500 and 1200 nm. The intensity of this band is always low in octahedral complexes and it is

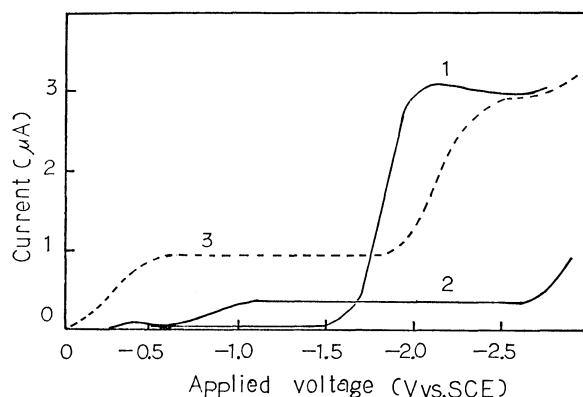


Fig. 5. D.c. polarograms of Co(II) and Co(III) complexes in DMSO.

1 and 2: $[(\text{acac})_2\text{Co}-\text{O}_2-\text{Co}(\text{acac})_2]^{2-}$,
3: $9 \times 10^{-4} \text{ mol dm}^{-3} \text{ Co}(\text{acac})_3$.

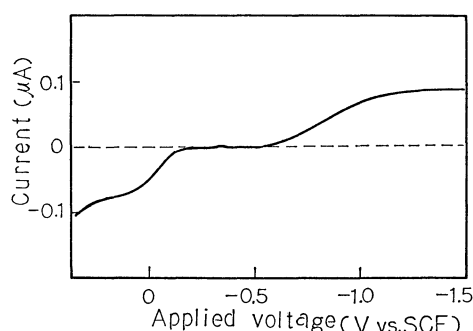


Fig. 6. D.c. polarogram of Co(II) complex in DMSO. Solution containing 0.05 mol dm^{-3} TBAP and μ -hyperoxo-dicobalt(II) complex.

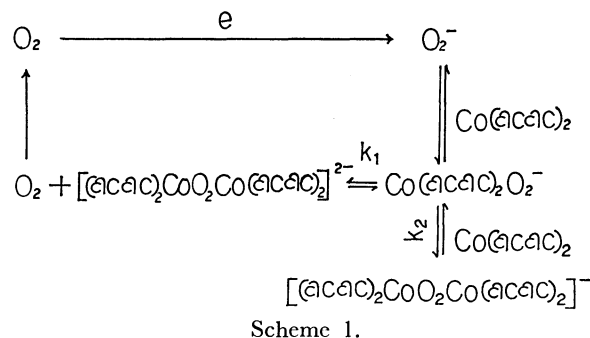
not known where the molar absorption coefficient exceeds $50 \text{ dm}^3 \text{ mol}^{-1} \text{ cm}^{-1}$.⁶⁾ It is known that the intensity in tetrahedral field is usually close to the molar absorption coefficient of $700 \text{ dm}^3 \text{ mol}^{-1} \text{ cm}^{-1}$.⁶⁾ On the other hand, the intensity at 588 nm for the $[(\text{dpm})_2\text{Co}-\text{O}_2-\text{Co}(\text{dpm})_2]^{2-}$ complex which has a square pyramidal structure^{5,7)} shows an intermediate intensity between that of tetrahedral and octahedral cobalt(II). The spectrophotometric profiles of the complexes A-1 and B-1 in the visible region are similar to the spectrum of the Co(II)-dpm complex (curve 3 in Fig. 4). Consequently, it appears that the two absorption bands at 17000 and 23000 cm^{-1} for the Co(II)-acac complexes in Fig. 4 are associated with a square pyramidal structure. From these results, we can consider A-1 and B-1 complexes as the same.

Typical polarograms of the above complex and tris(acetylacetonato)cobalt(III) complex are shown in Fig. 5. In Fig. 5, curves 1, 2, and 3 were obtained from a solution of the complexes, A-1, B-1, and $\text{Co}(\text{acac})_3$ containing about 0.05 mol dm^{-3} TBAP. In a DMSO medium, the $\text{Co}(\text{acac})_3$ complex undergoes stepwise reduction to Co(II) and Co(O). The half-wave potentials of the first $\text{Co(III)} \rightarrow \text{Co(II)}$ and the second $\text{Co(II)} \rightarrow \text{Co(O)}$ waves are -0.29 and -2.13 V vs. SCE . On the other side, for curve 1, the reduction wave at -1.8 V was caused by the reduction of aldol condensation products of acetone⁸⁾ in A-1. The complex did not show a reduction wave under

these conditions. For curve 2, the reduction wave at -0.85 V can be attributed to the presence of other complexes produced during the electrolysis, namely, the μ -peroxo-dicobalt(II) complex is unreducible.

In Fig. 6, the polarogram of the complex, A-2, is shown. This complex gives two waves in DMSO containing 0.05 mol dm^{-3} TBAP, the first half-wave potential at -0.05 V corresponding to oxidation to the $+3$ cobalt state and the second at -0.85 V probably corresponding to the reduction to the $[\text{Co}-\text{O}_2-\text{Co}]^{2-}$ state. The limiting currents of both waves were almost equal to each other and diffusion controlled. The second wave was characteristically irreversible and the half-wave potential was the more negative side than that of the oxygen molecule under the same conditions, thought to be due to the reduction of the bridging group, $-\text{O}_2-$, in the μ -hyperoxide-dicobalt(II) complex. Recently, it has become apparent that the catalytic electrode reaction consists of two distinct simultaneous chemical reactions. Accordingly, the μ -hyperoxo-dicobalt(II) complex may also be formed simultaneously. There is no doubt that such a reaction results in a lowering of the rate of the oxygen regeneration.

The catalytic electrode reaction mechanism has been estimated as follows:



In this scheme, the k_1 path occurred through a six coordinate intermediate, $[\text{Co}(\text{acac})_2\text{O}_2]^-$. Moreover, the k_1 path was easier than the k_2 path in aprotic solvents. Thus, in the k_2 path the releasing process of the solvent molecule in a solvated complex, $\text{Co}(\text{acac})_2(\text{sol})_2$ is the rate-determining step.

References

- 1) A. Iwase and S. Kudo, *Nippon Kagaku Kaishi*, **1976**, 42.
- 2) A. Iwase and S. Tada, *Nippon Kagaku Kaishi*, **1972**, 1828.
- 3) C. K. Mann and K. K. Barnes, "Electrochemical Reactions in Nonaqueous Systems," Marcel Dekker (1970), p. 497.
- 4) W. L. Jolly, *Inorg. Synth.*, **11**, 84 (1968).
- 5) A. Iwase and S. Kudo, Paper 9A714, 26th International Congress of Pure and Applied Chemistry, Tokyo, September 1977.
- 6) R. L. Carlin, "Transitional Metal Chemistry," Marcel Dekker (1966), Vol. 2, p. 149.
- 7) F. Lions, I. G. Dance, and J. Lewis, *J. Chem. Soc., A*, **1967**, 565.
- 8) J. Riddick and W. B. Bunger, "Techniques of Chemistry," Organic Solvents, Wiley-Interscience (1970), Vol. 2, p. 722.